Hindawi
Complexity
Volume 2018, Article ID 1696851, 11 pages
https://doi.org/10.1155/2018/1696851

Research Article

Neural Adaptive Sliding-Mode Control of a Bidirectional Vehicle Platoon with Velocity Constraints and Input Saturation

Maode Yan, Jiacheng Song, Panpan Yang, and Lei Zuo

School of Electronic and Control Engineering, Chang'an University, Xi'an, China

Correspondence should be addressed to Maode Yan; mdyan@chd.edu.cn

Received 14 May 2018; Accepted 8 August 2018; Published 2 December 2018

Academic Editor: Junpei Zhong

This paper investigates the vehicle platoon control problems with both velocity constraints and input saturation. Firstly, radial basis function neural networks (RBF NNs) are employed to approximate the unknown driving resistance of a vehicle's dynamic model. Then, a bidirectional topology, where vehicles can only communicate with their direct preceding and following neighbors, is used to depict the relationship among the vehicles in the platoon. On this basis, a neural adaptive sliding-mode control algorithm with an anti-windup compensation technique is proposed to maintain the vehicle platoon with desired distance. Moreover, the string stability and the strong string stability of the whole vehicle platoon are proven through the stability theorem. Finally, numerical simulations verify the feasibility and effectiveness of the proposed control method.

1. Introduction

The vehicle platoon, which means that all vehicles in a group communicate with each other and regulate their motion to reach the desired intervehicle distance, has received considerable attention in recent years [1, 2]. Its prominent advantages in enhancing traffic safety and improving highway capacity as well as reducing carbon emission have been well studied [3, 4].

Vehicle platoon control can be traced back to the PATH (Partners for Advanced Transit and Highways) program in the 1980s, in which many well-known issues are studied, such as control architecture, collision avoidance, and string stability [5–7]. Since then, many other topics on the vehicle platoon control have been discussed in terms of the range policy [8, 9], the communication topology [10–12], and the dynamic heterogeneity [13]. Moreover, some advanced platoon control algorithms have been proposed for the vehicle dynamics model under the framework of multiagent consensus control [3, 4] and the framework of sliding-mode control [14, 15]. However, most of them do not consider the realistic problems in terms of input saturation, velocity constraints, and model nonlinearities.

Actually, input saturation and velocity constraints are two important realistic problems in vehicle platoon systems, which may lead to performance degradation and instability of vehicles or even instability of the whole vehicle platoon system [16, 17]. Input saturation in the vehicle denotes that the throttle output characteristics of the vehicle are restricted subject to the physical limitations of actuators. And velocity constraints represent the discrepancy of velocity between actual reachability values and theoretical values, which are caused by throttle output characteristics, limitations of gearbox, and so on [18]. Actually, in many known algorithms, simulation results of velocity appear to have positive and negative shocks at the initial phase because of the random initial errors. However, this is the very last thing we needed or wanted. Thus, it is necessary to develop the study about vehicle platoon control with input saturation and velocity constraints. In fact, input saturation and velocity constraints have been studied independently in some literatures [19–22]. However, to the best of our knowledge, few studies take into account the influence of input saturation and velocity constraints simultaneously.

To solve the input saturation problem, a feasible approach is to add a smooth function $\tanh(\cdot)$ to the algorithm such that the proposed algorithm can exert great control effect on a single target [23–25]. For the platoon system, a similar method is used to design the distributed control algorithm such that the control inputs are limited in a specified range [26, 27]. However, the bounds of control inputs are associated with the number of vehicles in the platoon and the value of control gains in the above works. There is another method to deal with the input saturation considering needlessly the influence of the number of vehicles [28, 29]. In [28], a modified control design framework is presented to prevent the destroyed learning capabilities in the presence of input saturation and is extended for the control of an aircraft model. In [29], an adaptive coordinated control algorithm is proposed on the basis of [28] to control a multi-high-speed train system with input saturation. Moreover, literature that studies particularly the problem of velocity constraints in vehicle platoon control seems few. However, studies about state constraints of a cooperative control system in theory are a hot study area [19, 30, 31]. In [19], considering the influence of input or state constraints, a unified approach is proposed to analyze and design consensus control laws for a multiagent system. Discarded consensus algorithms are also effective methods to handle the problem of state or input constraints [32, 33].

Leveraging the above works, vehicles in the platoon are designed by only communicating with their direct preceding and following neighbors in this paper. And a neural adaptive sliding-mode control algorithm is proposed to handle the problems of vehicle platoon control with both input saturation and velocity constraints, simultaneously and systematically. The main features of this paper can be summarized as

(i) RBF NNs are used to learn online the unknown driving resistance such that it can be described in mathematics accurately. And the adaptive technique is used to estimate the optimal weight vectors in RBF NNs. In order to improve the robustness of the system, a sliding surface, which can reduce the disturbance from unknown driving resistance, is constructed

(ii) Considering the problems of vehicle platoon control with velocity constraints and input saturation, an anti-windup compensation method is utilized to attenuate the integral windup of the adaptive control laws and velocity. Furthermore, a neural adaptive sliding-mode control algorithm is proposed to guarantee the string stability (Definition 1) and the strong string stability (Definition 2) of the whole vehicle platoon

The remainder of this paper is organized as follows. The preliminaries and the problem formulation are described in Section 2. In Section 3, the control algorithms of vehicle platoon systems are proposed. Simulations are performed in Section 4 to demonstrate the effectiveness of our algorithms. The conclusion is given in Section 5.

2. Problem Formulation and Preliminaries

Consider a vehicle platoon with following longitudinal dynamics:

$$\begin{cases} \dot{r}_i(t) = v_i(t), \\ M_i \dot{v}_i(t) = F_i(t) - f_i(r_i, v_i, t), \\ \quad i = 1, 2, \ldots, n, \end{cases} \tag{1}$$

where M_i is the mass of the ith vehicle. $r_i(t)$ and $v_i(t)$ denote the position and velocity, respectively, of the ith vehicle. $F_i(t)$ represents the actuator force of the ith vehicle. In addition, $f_i(r_i, v_i, t)$ describes the unknown driving resistance.

In order to simplify the design process of the controller, the dynamics of the vehicle can be rewritten as

$$\begin{cases} \dot{r}_i(t) = v_i(t), \\ \dot{v}_i(t) = u_i(t) - g_i(r_i, v_i, t), \\ \quad i = 1, 2, \ldots, n, \end{cases} \tag{2}$$

where $u_i(t) \coloneqq F_i(t)/M_i$, $g_i(r_i, v_i, t) \coloneqq f_i(r_i, v_i, t)/M_i$.

In practice, the control inputs and velocities of vehicles are curbed because of the physical constraints of the actuator. In order to show the saturation characteristic in vehicle dynamics, the control input $u_i(t)$ and the velocity $v_i(t)$ with saturation are described in the following form:

$$\begin{aligned} u_{i0}(t) &= \mathrm{sat}(u_{\min}, u_i(t), u_{\max}) \\ &= \begin{cases} u_{\min}, & \text{if } u_i(t) < u_{\min}, \\ u_i(t), & \text{if } u_{\min} \le u_i(t) \le u_{\max}, \\ u_{\max}, & \text{if } u_i(t) > u_{\max}, \end{cases} \end{aligned} \tag{3a}$$

$$\begin{aligned} v_{i0}(t) &= \mathrm{sat}(v_{\min}, v_i(t), v_{\max}) \\ &= \begin{cases} v_{\min}, & \text{if } v_i(t) < v_{\min}, \\ v_i(t), & \text{if } v_{\min} \le v_i(t) \le v_{\max}, \\ v_{\max}, & \text{if } v_i(t) > v_{\max}, \end{cases} \end{aligned} \tag{3b}$$

where $u_{i0}(t)$, the saturated control input, is the real control input used in the controller. $v_{i0}(t)$ denotes the constrained velocity. $u_{\min}$ and $u_{\max}$ are known constants, which represent the bounds of the control force. $v_{\min}$ and $v_{\max}$ denote the bounds of the vehicle's velocity.

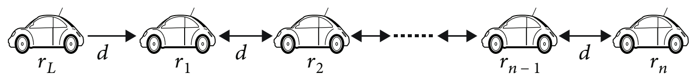

Figure 1: Bidirectional topology of the vehicle platoon.

Then, the dynamics of vehicle can be rewritten as

$$\begin{cases} \dot{r}_i(t) = v_i(t), \\ \dot{v}_i(t) = u_i(t) - g_i(r_i, v_i, t), \\ u_i(t) = u_{i0}(t), \\ v_i(t) = v_{i0}(t), \\ \quad i = 1, 2, \ldots, n. \end{cases} \tag{4}$$

The structure of the vehicle platoon is described by Figure 1 which consists of a leader and n followers. Bidirectional topology is adopted to ensure that every vehicle in the platoon communicates with its neighboring preceding and following vehicles in this paper.

Remark 1. Bidirectional topology means that only the information of the forward and backward vehicles are transferred to the target vehicle by communication facilities. In other words, bidirectional topology can reduce the complexity of communication among the vehicles in the platoon compared with other topologies used in algorithms under the framework of multiagent consensus control (the information of every vehicle in the platoon is needed). Consequently, the communication load of the proposed algorithm is reduced.

The main control objectives of this paper can be described as follows:

(i) The string stability of the vehicle platoon system can be guaranteed, which means that (1) the position tracking error of each vehicle in the platoon is kept bounded, i.e., $e_{r,i} = r_{i-1} - r_i - d \le \rho$, where ρ is a small positive constant, d indicates the prespecified distance between two intervehicles, and $e_{r,i}$ represents the position tracking error and (2) the Lyapunov functions of individual vehicle and whole vehicle platoon system satisfy the stability proof

(ii) The strong string stability of the whole platoon system can be guaranteed, i.e., $|e_{r,n}| \le |e_{r,n-1}| \le \cdots \le |e_{r,1}|$

(iii) The control input and velocity of each vehicle are limited in the reachable range

To this end, the following definitions, assumptions, and lemmas are used throughout the paper.

Assumption 1. The desired velocity v_L and its derivative $\dot{v}_L$ are known and bounded.

Assumption 2 [34]. The $g_i(r_i, v_i, t)$ is an unknown bounded smooth function.

Remark 2. Assumptions 1 and 2 are standard conditions required in many control schemes, which can be commonly found in the existing literature [35].

Definition 1 [36] (string stability). Origin $e_{r,i} = 0$ with vehicle dynamics modeled by (10) is string stable, if given any $\iota > 0$. There exists $\sigma > 0$ such that

$$\left\| e_{r,i}(0) \right\|_\infty < \sigma \Rightarrow \sup_i \left\| e_{r,i}(\cdot) \right\|_\infty < \iota, \quad i = 1, 2, \ldots, n. \tag{5}$$

Definition 2 [37] (strong string stability). Origin $e_{r,i} = 0$ with each vehicle's dynamics modeled by (10) is strong string stable if error propagation transfer function $G_i(s) \coloneqq E_{i+1}(s)/E_i(s)$ satisfies $|G_i(s)| < 1$ for all $i = 1, 2, \ldots, n$.

Lemma 1 [38]. *There is a continuous function $V(t) \ge 0$, and $V(0)$ is bounded. Then, $V(t)$ is bounded if the following inequality holds:*

$$\dot{V}(t) \le -p_1 V(t) + p_2, \tag{6}$$

where $p_1 > 0$ and p_2 are constants.

Lemma 2 [39, 40]. *RBF NNs can approximate online an unknown smooth function $Q(z)$ in the form of $Q(z) = W^T \Psi(z)$, where $z \in R^q$ denotes the input of the neural network and q represents the dimension of the neural network input. $W = [w_1, w_2, \ldots, w_m]^T$, where w_l is the parameter vector and m indicates the number of neurons. $\Psi(z) = [\varphi_1(z) \cdots \varphi_m(z)]^T$, where $\varphi_l(z)$ is Gaussian functions*

$$\varphi_l(z) = \exp\left(\frac{-(z - \mu_l)^T (z - \mu_l)}{\eta_l^2} \right), \quad l = 1, 2, \ldots, m, \tag{7}$$

where μ_l and η_l are the centers and widths, respectively, of the Gaussian functions. RBF NNs can approximate $Q(z)$ to arbitrary accuracy by setting numerous hidden neurons

$$Q(z) = W^{*T} \Psi(z) + \varepsilon(z). \tag{8}$$

The approximation error $\varepsilon(z)$ can be arbitrarily adjusted to be small by choosing the ideal bounded weight vector. And $|\varepsilon(z)| \le \bar{\varepsilon} \le \infty$ is a small positive constant

$$W^* \coloneqq \arg \min_{W \subset R^q} \left\{ \sup_{z \in \Omega_z} \left| Q(z) - W^T \Psi(z) \right| \right\}. \tag{9}$$

3. Main Results

In this section, we will give the detail steps of the controller design. First step: RBF NNs are adopted to establish the model of the vehicle, and the sliding surface is further constructed; second step: the platoon system is constructed based on bidirectional topology; third step: a neural adaptive sliding-mode algorithm is proposed to handle the velocity constraints and input saturation for a vehicle platoon.

3.1. First Step: Establish the Vehicle Model Based on RBF NNs and Construct the Sliding Surface. In order to estimate the unknown driving resistance, RBF NNs are adopted to approximate online the $g_i(r_i, v_i, t)$, and we further establish the model

$$\dot{v}_i(t) = u_i(t) - W_i^* \Psi_i(z) - \varepsilon_i(z), \tag{10}$$

where z denotes the input of RBF NNs and $z = [e_{r,i}, \dot{e}_{r,i}]$. $e_{r,i}$ represents the position tracking error of the ith vehicle and is defined as

$$e_{r,i} = r_{i-1} - r_i - d, \tag{11}$$

where d indicates the prespecified distance between two intervehicles.

To overcome the degradation of system transient performance caused by large nonzero initial position tracking error, a modified tracking error is defined as

$$\bar{e}_{r,i}(t) = e_{r,i}(t) - \chi_i(t), \tag{12}$$

with

$$\chi_i(t) = [e_{r,i}(0) + (\zeta_i e_{r,i}(0) + \dot{e}_{r,i}(0))t]e^{-\zeta_i t}, \tag{13}$$

where $e_{r,i}(0) = e_{r,i}(t)|_{t=0}$, $\dot{e}_{r,i}(0) = \dot{e}_{r,i}(t)|_{t=0}$ and ζ_i is a positive constant. Thus, we have

$$\begin{aligned} \bar{e}_{r,i}(t)|_{t=0} &= 0, \\ \dot{\bar{e}}_{r,i}(t)|_{t=0} &= 0. \end{aligned} \tag{14}$$

It is obvious that $\bar{e}_{r,i}(t)$ converges to $e_{r,i}(t)$ when $\chi_i(t)$ converges to zero, where the rate of convergence is determined by ζ_i. In addition, in order to improve the robustness of the proposed controller, a sliding surface is constructed as

$$s_i = \dot{\bar{e}}_{r,i} + \alpha_i \bar{e}_{r,i}, \tag{15}$$

where α_i is a positive constant. It is known that the convergence and boundness of the sliding surface s_i and $\bar{e}_{r,i}(t)$ are equivalent.

Remark 3. The importance of $\chi_i(t)$ is that it can transform the nonzero initial position tracking error problem to a zero initial position tracking error problem. And it can make that all the system states are on the sliding hyperplane at the initial instant, i.e., $s_i(0) = 0$. As a result, the reaching phase of the sliding-mode control is eliminated and the transient response of the system is improved.

3.2. Second Step: Construct the Bidirectional Communication Topology. It is worth noting that (15) only describes the dynamic characteristics of a single vehicle. To describe the stability of the whole platoon, we adopt the coupled sliding surface (CSS) to establish the relationship between the ith and the $(i+1)$th vehicle:

$$S_i = \beta_i s_i - s_{i+1}. \tag{16}$$

It is clear that s_{n+1} does not exist, so we set $s_{n+1} = 0$, then, $S_n = \beta_n s_n$. Furthermore, we define matrices $\mathbf{S}_1 = [s_1, s_2, \ldots, s_n]^T$ and $\mathbf{S}_2 = [S_1, S_2, \ldots, S_n]^T$ to depict the total vehicle platoon system. The relationship between $\mathbf{S}_1$ and $\mathbf{S}_2$ can be described as

$$\mathbf{S}_2 = \mathbf{B}\mathbf{S}_1, \tag{17}$$

where

$$\mathbf{B} = \begin{bmatrix} \beta_1 & -1 & 0 & \cdots & 0 \\ 0 & \beta_2 & -1 & \cdots & 0 \\ \vdots & \vdots & \vdots & \ddots & \vdots \\ 0 & 0 & 0 & \cdots & -1 \\ 0 & 0 & 0 & \cdots & \beta_n \end{bmatrix}. \tag{18}$$

It is necessary to know that the parameter β_i, $i = 1, 2, \ldots, n$, can be designed. If we choose $\beta_i > 0$, the matrix $\mathbf{B}$ is nonsingular. Thus, the asymptotic convergence and the ultimate boundedness of S_i are equivalent to s_i.

Therefore, taking the time derivative of S_i in (16) yields

$$\begin{aligned} \dot{S}_i &= \beta_i \dot{s}_i - \dot{s}_{i+1} = \beta_i \left(\ddot{\bar{e}}_{r,i} + \alpha_i \dot{\bar{e}}_{r,i}\right) - \left(\ddot{\bar{e}}_{r,i+1} + \alpha_{i+1} \dot{\bar{e}}_{r,i+1}\right) \\ &= \beta_i (\ddot{r}_{i-1} - \ddot{r}_i - \ddot{\chi}_i + \alpha_i (\dot{r}_{i-1} - \dot{r}_i - \dot{\chi}_i)) \\ &\quad - (\ddot{r}_i - \ddot{r}_{i+1} - \ddot{\chi}_{i+1} + \alpha_{i+1} (\dot{r}_i - \dot{r}_{i+1} - \dot{\chi}_{i+1})) \\ &= -(\beta_i + 1)(u_i(t) - W_i^* \Psi_i(z) - \varepsilon_i(z)) + D_i, \end{aligned} \tag{19}$$

where $D_i = \beta_i (\ddot{r}_{i-1} - \ddot{\chi}_i + \alpha_i (\dot{r}_{i-1} - \dot{r}_i - \dot{\chi}_i)) - (-\ddot{r}_{i+1} - \ddot{\chi}_{i+1} + \alpha_{i+1} (\dot{r}_i - \dot{r}_{i+1} - \dot{\chi}_{i+1}))$.

Particularly, we know that $S_n = \beta_n s_n$ when $i = n$. The time derivative of S_n can be written as

$$\begin{aligned} \dot{S}_n &= \beta_n \dot{s}_n = \beta_n \left(\ddot{\bar{e}}_{r,n} + \alpha_n \dot{\bar{e}}_{r,n}\right) \\ &= \beta_n (\ddot{r}_{n-1} - \ddot{r}_n - \ddot{\chi}_n + \alpha_n (\dot{r}_{n-1} - \dot{r}_n - \dot{\chi}_n)) \\ &= -\beta_n (u_n(t) - W_n^* \Psi_n(z) - \varepsilon_n(z)) + D_n, \end{aligned} \tag{20}$$

where $D_n = \beta_n (\ddot{r}_{n-1} - \ddot{\chi}_n + \alpha_n (\dot{r}_{n-1} - \dot{r}_n - \dot{\chi}_n))$.

Remark 4. It is clear that CSS includes the information from the neighbor vehicles (direct predecessor and direct follower) of (19) and (20). It means that the CSS achieves the bidirectional topology for vehicle platoon.

3.3. Third Step: Design the Control Algorithm by Considering the Velocity Constraints and Input Saturation. Actually, the velocity constraints and input saturation appear frequently in application and have been proven to be the main source of performance degradation [41]. To overcome the degradation of system transient performance caused by saturation, an anti-windup compensator method is utilized to modify the tracking error. The signal $\phi_i(t)$ is generated as the output of the following equation:

$$\dot{\phi}_i(t) = -\psi_i\phi_i(t) + (\beta_i + 1)(u_{i0}(t) - u_i(t)), \tag{21a}$$

$$\dot{\phi}_n(t) = -\psi_n\phi_n(t) + \beta_n(u_{n0}(t) - u_n(t)). \tag{21b}$$

Let $\delta_i(t) = S_i(t) - \phi_i(t)$. The new tracking error can be written as

$$\begin{aligned}\dot{\delta}_i &= -(\beta_i + 1)(u_i - W_i^*\Psi_i(z) - \varepsilon_i(z)) \\ &\quad - (\beta_i + 1)(u_{i0} - u_i) + D_i + \psi_i\phi_i \\ &= -(\beta_i + 1)\left(u_{i0} - \Theta_i^{\mathrm{T}}\mathbf{H}_i\right) + D_i + \psi_i\phi_i,\end{aligned} \tag{22a}$$

$$\begin{aligned}\dot{\delta}_n &= -\beta_n(u_n - W_n^*\Psi_n(z) - \varepsilon_n(z)) + D_n \\ &\quad - \beta_n(u_{n0} - u_n) + \psi_n\phi_n \\ &= -\beta_n\left(u_{n0} - \Theta_n^{\mathrm{T}}\mathbf{H}_n\right) + D_n + \psi_n\phi_n,\end{aligned} \tag{22b}$$

where $\mathbf{H}_i = [\Psi_i(z), 1]^{\mathrm{T}}$, $\Theta_i^{\mathrm{T}} = [W_i^*, \varepsilon_i(z)]$, $\mathbf{H}_n = [\Psi_n(z), 1]^{\mathrm{T}}$, and $\Theta_n^{\mathrm{T}} = [W_n^*, \varepsilon_n(z)]$.

Remark 5. The function of the signal $\phi_i(t)$ is to attenuate the integral windup of the control law and velocity when velocity constraints or input saturation occur. In case of velocity constraints or input saturation ($v_{i0} - v_i \neq 0$ or $u_{i0} - u_i \neq 0$), the signal S_i will rise and the constructed signal $\phi_i(t)$ will also rise, which, in turn, ensures that the newly defined tracking error $\delta_i(t)$ cannot rise abruptly.

In addition, for the signal $\phi_i(t)$, we have the following lemma.

Lemma 3 *For the signal $\phi_i(t)$, it holds for the following equation for any $t > 0$:*

$$|\phi_i(t)| \leq |Z_i| + \varpi_i, \quad i = 1, 2, \ldots, n, \tag{23}$$

where $Z_i = ((\beta_i + 1)(u_{i0} - u_i))/\psi_i$. ϖ_i is a positive constant.

Proof. The output of (21a) and (21b) can be described as

$$\begin{aligned}\phi_i(t) &= \phi_i(0)e^{-\psi_i t} + Z_i e^{-\psi_i t}\int_0^t e^{\psi_i\varpi}d\varpi \\ &= \phi_i(0)e^{-\psi_i t} + Z_i\left(1 - e^{-\psi_i t}\right).\end{aligned} \tag{24}$$

From (24), we know that $|\phi_i(t)| \leq |Z_i|$ as $t \to \infty$. Thus, for any $t > 0$, if there exists a positive scalar ϖ_i, $|\phi_i(t)| \leq |Z_i| + \varpi_i$ can be ensured, i.e., $\phi_i(t)$ is bounded.

Furthermore, the control law of the ith vehicle is formulated as

$$\begin{aligned}u_i(t) &= \frac{k_1}{\beta_i + 1}\delta_i + \frac{1}{\beta_i + 1}D_i + \widehat{\Theta}_i^{*T}\mathbf{H}_i \\ &\quad + \frac{1}{\beta_i + 1}\psi_i\phi_i, \quad i = 1, 2, \ldots, n - 1,\end{aligned} \tag{25}$$

where $\Theta_i^{*T} = [W_i^*, \bar{\varepsilon}_i]$ and $\widehat{\Theta}_i^{*T} = [\widehat{W}_i^*, \widehat{\bar{\varepsilon}}_i]$. $\widehat{W}_i^*$ and $\widehat{\bar{\varepsilon}}_i$ represent the estimated value of W_i^* and $\bar{\varepsilon}_i$, respectively. It is necessary to point out that $\varepsilon_i(z) \leq \bar{\varepsilon}_i$ and $\bar{\varepsilon}_i$ is a small positive constant.

The control law of the nth vehicle is designed as

$$u_n(t) = \frac{k_2}{\beta_n}\delta_n + \frac{1}{\beta_n}D_n + \widehat{\Theta}_n^{*T}\mathbf{H}_n + \frac{1}{\beta_n}\psi_n\phi_n, \tag{26}$$

where $\Theta_n^{*T} = [W_n^*, \bar{\varepsilon}_n]$ and $\widehat{\Theta}_n^{*T} = [\widehat{W}_n^*, \widehat{\bar{\varepsilon}}_n]$. $\widehat{W}_n^*$ and $\widehat{\bar{\varepsilon}}_n$ represent the estimated value of W_n^* and $\bar{\varepsilon}_n$, respectively. $\varepsilon_n(z) \leq \bar{\varepsilon}_n$ and $\bar{\varepsilon}_n$ is a small positive constant.

The results about the vehicle platoon with velocity constraints and input saturation are as follows.

Theorem 1 *Consider a vehicle platoon modeled as (10) with velocity constraints and input saturation. The proposed control laws (3a) and (3b), (25), and (26) are used to control each vehicle. In addition, we design the following adaptive estimation laws:*

$$\dot{\widehat{\Theta}}_i^* = \Gamma_1\left((\beta_i + 1)\mathbf{H}_i\delta_i - \xi_{1i}\widehat{\Theta}_i^*\right), \quad i = 1, 2, \ldots, n - 1, \tag{27a}$$

$$\dot{\widehat{\Theta}}_n^* = \Gamma_2\left(\beta_n\mathbf{H}_n\delta_n - \xi_{1n}\widehat{\Theta}_n^*\right), \tag{27b}$$

where ξ_{1i}, ξ_{1n}, $\Gamma_1 = [\lambda_i^1, \lambda_i^2]^{\mathrm{T}}$, and $\Gamma_2 = [\lambda_n^1, \lambda_n^2]^{\mathrm{T}}$ are the parameters to be designed. Then, we have the following results:

(i) The new tracking error $\delta_i(t)$, coupled sliding surface S_i, and position tracking error $e_{r,i}$ will converge to an arbitrarily small value

(ii) Meanwhile, the stability of each vehicle in the platoon and the string stability of the total vehicle platoon system can be guaranteed

(iii) The strong string stability of the vehicle platoon can be ensured, i.e., $|e_{r,n}| \leq |e_{r,n-1}| \leq \cdots \leq |e_{r,1}|$

Proof. For the case $(u_i - u_{i0} \neq 0)$ or $(v_i - v_{i0} \neq 0)$, the vehicles move under the control inputs (25) and (26). We design the following Lyapunov function candidate:

$$V = \sum_{i=1}^{n} V_i, \tag{28a}$$

$$V_i = \frac{1}{2}\delta_i^2 + \frac{1}{2}\tilde{\Theta}_i^{*\mathrm{T}}\Gamma_1^{-1}\tilde{\Theta}_i^{*}, \tag{28b}$$

where $\tilde{\Theta}_i^{*\mathrm{T}} = [\widehat{W}_i^* - W_i^*, \widehat{\bar{\varepsilon}}_i - \bar{\varepsilon}_i]$, $i = 1, 2, \dots, n$.

Taking the time derivative of (28b), it follows

$$\begin{aligned}
\dot{V}_i &= \delta_i\dot{\delta}_i + \tilde{\Theta}_i^{*T}\Gamma_1^{-1}\dot{\tilde{\Theta}}_i^{*T} = \delta_i\Bigg(-(\beta_i+1)\bigg(\frac{k_1}{\beta_i+1}\delta_i \\
&\quad + \widehat{\Theta}_i^{*T}\mathbf{H}_i - \Theta_i^T\mathbf{H}_i + \frac{1}{\beta_i+1}D_i + \frac{1}{\beta_i+1}\psi_i\phi_i\bigg) \\
&\quad + D_i + \psi_i\phi_i\Bigg) + \tilde{\Theta}_i^{*T}\Gamma_1^{-1}\dot{\tilde{\Theta}}_i^{*T} \\
&\le \delta_i\Bigg(-(\beta_i+1)\bigg(\frac{k_1}{\beta_i+1}\delta_i + \widehat{\Theta}_i^{*T}\mathbf{H}_i - \Theta_i^{*T}\mathbf{H}_i \\
&\quad + \frac{1}{\beta_i+1}D_i + \frac{1}{\beta_i+1}\psi_i\phi_i\bigg) + D_i + \psi_i\phi_i\Bigg) + \tilde{\Theta}_i^{*T}\Gamma_1^{-1}\dot{\tilde{\Theta}}_i^{*T} \\
&= -k_1\delta_i^2 - (\beta_i+1)\delta_i\tilde{\Theta}_i^{*T}\mathbf{H}_i + \tilde{\Theta}_i^{*T}\Gamma_1^{-1}\dot{\tilde{\Theta}}_i^{*T} \\
&= -k_1\delta_i^2 - \xi_{1i}\tilde{\Theta}_i^{*T}\widehat{\Theta}_i^{*}, \quad i = 1, 2, \dots, n-1.
\end{aligned} \tag{29}$$

Particularly, when $i = n$, the time derivative of (28b) can be written as

$$\begin{aligned}
\dot{V}_n &= \delta_n\dot{\delta}_n + \tilde{\Theta}_n^{*T}\Gamma_2^{-1}\dot{\tilde{\Theta}}_n^{*T} = \delta_n\Bigg(-\beta_n\bigg(\frac{k_2}{\beta_n}\delta_n \\
&\quad + \widehat{\Theta}_n^{*T}\mathbf{H}_n - \Theta_n^T\mathbf{H}_n + \frac{1}{\beta_n}D_n + \frac{1}{\beta_n}\psi_n\phi_n\bigg) \\
&\quad + D_n + \psi_n\phi_n\Bigg) + \tilde{\Theta}_n^{*T}\Gamma_2^{-1}\dot{\tilde{\Theta}}_n^{*T} \\
&\le \delta_n\Bigg(-\beta_n\bigg(\frac{k_2}{\beta_n}\delta_n + \widehat{\Theta}_n^{*T}\mathbf{H}_n - \Theta_n^{*T}\mathbf{H}_n + \frac{1}{\beta_n}D_n \\
&\quad + \frac{1}{\beta_n}\psi_n\phi_n\bigg) + D_n + \psi_n\phi_n\Bigg) + \tilde{\Theta}_n^{*T}\Gamma_2^{-1}\dot{\tilde{\Theta}}_n^{*T} \\
&= -k_2\delta_n^2 - \xi_{1n}\tilde{\Theta}_n^{*T}\widehat{\Theta}_n^{*}.
\end{aligned} \tag{30}$$

According to the Young's inequality, we have

$$-\xi_{1i}\tilde{\Theta}_i^{*T}\widehat{\Theta}_i^{*} = -\xi_{1i}\tilde{\Theta}_i^{*T}\left(\Theta_i^* + \tilde{\Theta}_i^*\right) \le \frac{\xi_{1i}\Theta_i^{*T}\Theta_i^*}{2} - \frac{\xi_{1i}\tilde{\Theta}_i^{*T}\tilde{\Theta}_i^*}{2}. \tag{31}$$

Then, (29) and (30) can be written as

$$\dot{V}_i \le -k_1\delta_i^2 + \frac{\xi_{1i}\Theta_i^{*T}\Theta_i^*}{2} - \frac{\xi_{1i}\tilde{\Theta}_i^{*T}\tilde{\Theta}_i^*}{2}, \quad i = 1, 2, \dots, n-1, \tag{32a}$$

$$\dot{V}_n \le -k_2\delta_n^2 + \frac{\xi_{1n}\Theta_n^{*T}\Theta_n^*}{2} - \frac{\xi_{1n}\tilde{\Theta}_n^{*T}\tilde{\Theta}_n^*}{2}, \quad i = n. \tag{32b}$$

Meanwhile, choose $\|\Gamma_1\| > 2$ and $\|\Gamma_2\| > 2$ and further define

$$\begin{aligned}
\varphi_i &= \frac{\xi_{1i}\Theta_i^{*T}\Theta_i^*}{2}, \\
\varphi_n &= \frac{\xi_{1n}\Theta_n^{*T}\Theta_n^*}{2},
\end{aligned} \tag{33a}$$

$$\begin{aligned}
\gamma_{1i} &= \min\left\{k_1, \frac{\xi_{1i}}{2}\right\}, \\
\gamma_{1n} &= \min\left\{k_2, \frac{\xi_{1n}}{2}\right\},
\end{aligned} \tag{33b}$$

$$\begin{aligned}
\gamma_{2i} &= \max\left\{\frac{1}{2}, \frac{\|\Gamma_1^{-1}\|}{2}\right\}, \\
\gamma_{2n} &= \max\left\{\frac{1}{2}, \frac{\|\Gamma_2^{-1}\|}{2}\right\}.
\end{aligned} \tag{33c}$$

Then

$$\dot{V}_i \le -\frac{\gamma_{1i}}{\gamma_{2i}}V_i + \varphi_i = -\omega_1 V_i + \varphi_i, \tag{34a}$$

$$\dot{V}_n \le -\frac{\gamma_{1n}}{\gamma_{2n}}V_n + \varphi_n = -\omega_2 V_n + \varphi_n, \tag{34b}$$

where $\omega_1 = \gamma_{1i}/\gamma_{2i}$ and $\omega_2 = \gamma_{1n}/\gamma_{2n}$.

According to Lemma 1, we know that V_i is bounded. And $V_i \le V_i(0) + (\varphi_i/\omega)$ (when $i = 1, 2, \dots, n-1$, $\omega = \omega_1$; $i = n$, $\omega = \omega_2$) with $V_i(0)$ being the initial value of V_i when $t \to \infty$. Furthermore, we can know that the signal δ_i and the coefficient estimation error $\tilde{\Theta}_i^*$ converge to the following compact set:

$$\frac{1}{2}\delta_i^2 \le V_i(0) + \frac{\varphi_i}{\omega} \Rightarrow |\delta_i| \le \sqrt{2V_i(0) + \frac{2\varphi_i}{\omega}}, \tag{35a}$$

$$\left|\tilde{\Theta}_i^*(j)\right| \le \sqrt{2\lambda_i^j V_i(0) + \frac{2\lambda_i^j\varphi_i}{\omega}}, \quad j = 1, 2. \tag{35b}$$

This implies that the tracking performance and stability of each vehicle can be guaranteed. Meanwhile, the estimation error of driving resistance can be limited to a bounded value. Then, for the string stability of the vehicle platoon, the time derivative of global Lyapunov candidates is written as

$$\dot{V} \le -\omega\sum_{i=1}^{n}V_i + \sum_{i=1}^{n}\varphi_i = -\omega V + \sum_{i=1}^{n}\varphi_i. \tag{36}$$

Therefore,

$$0 \le V \le \frac{\sum_{i=1}^{n}\varphi_i}{\omega} + \exp^{-\omega t}\left(V(0) - \frac{\sum_{i=1}^{n}\varphi_i}{\omega}\right). \tag{37}$$

Table 1: Control parameters of the vehicles ($i = 1, 2, \ldots, 7$).

α_i	β_i	ψ_i	$u_{\min}$	$u_{\max}$	$v_{\min}$	$v_{\max}$	ζ_i	ε_{1i}	$\Gamma_1 = \Gamma_2$	$k_1 = k_2$
0.2	0.9999	100	−1.3	1.3	0	13	0.5	0.005	[18,2]	8

Furthermore,

$$|\delta_i| \le \sqrt{\frac{2\sum_{i=1}^{n}\varphi_i}{\omega} + 2\exp^{-\omega t}\left(V(0) - \frac{\sum_{i=1}^{n}\varphi_i}{\omega}\right)}. \tag{38}$$

Thus,

$$|\delta_i| \le \sqrt{\frac{2\sum_{i=1}^{n}\varphi_i}{\omega} + 2V(0)} = B^+, \tag{39}$$

where B^+ is a positive constant.

From the above analysis, it can be seen that $\delta_i(t)$ will be limited in the range of 0 to B^+. Therefore, we know that S_i will be limited in the range of 0 to $(B^+ + \phi_i)$, which can be adjusted to an arbitrary small value by designing the ideal parameters χ_i and ξ_{1i}. It means that the string stability of the vehicle platoon is guaranteed.

Next, we will prove the strong string stability of the total vehicle platoon system. Since $S_i = \beta_i s_i - s_{i+1} = B^+ + |Z_i^*| + \varpi_i$, we can get

$$\beta_i(\dot{e}_{r,i} + \alpha_i e_{r,i}) = \left(\dot{e}_{r,i_1} + \alpha_{i+1}e_{r,i+1}\right) + B^+ + |Z_i^*| + \varpi_i. \tag{40}$$

Taking the Laplace transform of (40), it follows that

$$\begin{aligned}&\beta_i(sE_{r,i}(s) + \alpha_i E_{r,i}(s))\\ &\quad = B^+ + |Z_i^*| + \varpi_i + \left(sE_{r,i_1+1}(s) + \alpha_{i+1}E_{r,i+1}(s)\right).\end{aligned} \tag{41}$$

Letting $\alpha_i = \alpha_{i+1}$, we have

$$G_i(s) = \frac{E_{r,i+1}(s)}{E_{r,i}(s)} \le \frac{(s + \alpha_{i+1})E_{r,i+1}(s) + B^+ + |Z_i^*| + \varpi_i}{(s + \alpha_i)E_{r,i}(s)} = \beta_i, \tag{42}$$

where $B^+ + |Z_i^*| + \varpi_i > 0$.

Thus, the strong string stability can be guaranteed if β_i satisfies $0 < |\beta_i| < 1$.

4. Numerical Simulations

To evaluate the effectiveness and feasibility of the developed platoon control approaches, numerical simulations are performed in this section. We apply the designed algorithms to an 8-vehicle platoon with one leader and 7 followers.

4.1. Simulation Setup. The prespecified velocity profiles are described as

$$\begin{cases} v_L(t) = 10\sin(0.025t), & \text{if } t \le 20,\\ v_L(t) = 10, & \text{if } 20 < t \le 40,\\ v_L(t) = 10 + 3\sin(0.1t), & \text{if } 40 < t \le 60,\\ v_L(t) = 10, & \text{if } 60 < t \le 80,\\ v_L(t) = 10\sin(0.025t), & \text{if } 80 < t \le 100. \end{cases} \tag{43}$$

The desired distance between two consecutive vehicles is set to be $d = 10$ m (which can be set to be arbitrary values according to actual requirements). Each vehicle's initial values of velocity and position are set as $v_i = [0, 0, 0, 0, 0, 0, 0]$ and $r_i = [60, 48, 40, 28, 20, 8, 0]$, respectively. The leader's initial values of velocity and position are set as $v_L = 0$ and $r_L = 71$, respectively. Meanwhile, the driving resistance of each vehicle is designed as $g_i = 0.1(\sin(0.1\pi t))$. Furthermore, the neural networks used in this simulation contain 5 neurons, where $\eta_l = 0.5$ and $\mu_l = [-1, -0.5, 0, 0.5, 1]$. The other values are set to be zero. The control parameters are listed in Table 1.

4.2. Simulation Results and Discussion

Case 1. Vehicle platoon control with velocity constraints and input saturation.

The simulation results using the proposed algorithms (3a) and (3b), (25), and (26) are shown in Figure 2. The tracking performance of velocity in Figures 2(a) and 2(b) is excellent, and each vehicle in the platoon moves stably with acceptable velocity error (the biggest velocity error is 0.4 m/s in the adjustment phase and is adjusted to a small number close to zero, eventually). Meanwhile, from the local enlarged drawing in Figure 2(a), the values of velocity of the vehicles are positive, which satisfy the actual operation conditions.

Furthermore, it can be seen from Figures 2(c) and 2(d) that the distance between two vehicles converges to the desired values of 10 m and the position tracking error is adjusted to a small number close to zero. What is more, from the local enlarged drawing in Figure 2(d), we know that the strong string stability of the vehicle platoon can be achieved, i.e., $|e_{r,7}| \le |e_{r,6}| \le \cdots \le |e_{r,1}|$, and this advantage benefits from the CSS with $\beta_i < 1$.

Figure 2(e) shows the control input curves. It is clear that the control input can be limited in a desired range ($-1.3\,\text{m/s}^2$–$1.3\,\text{m/s}^2$). Figure 2(f) shows the estimated uncertain driving resistance using RBF NNs, and the performance of estimated uncertain driving resistance is excellent.

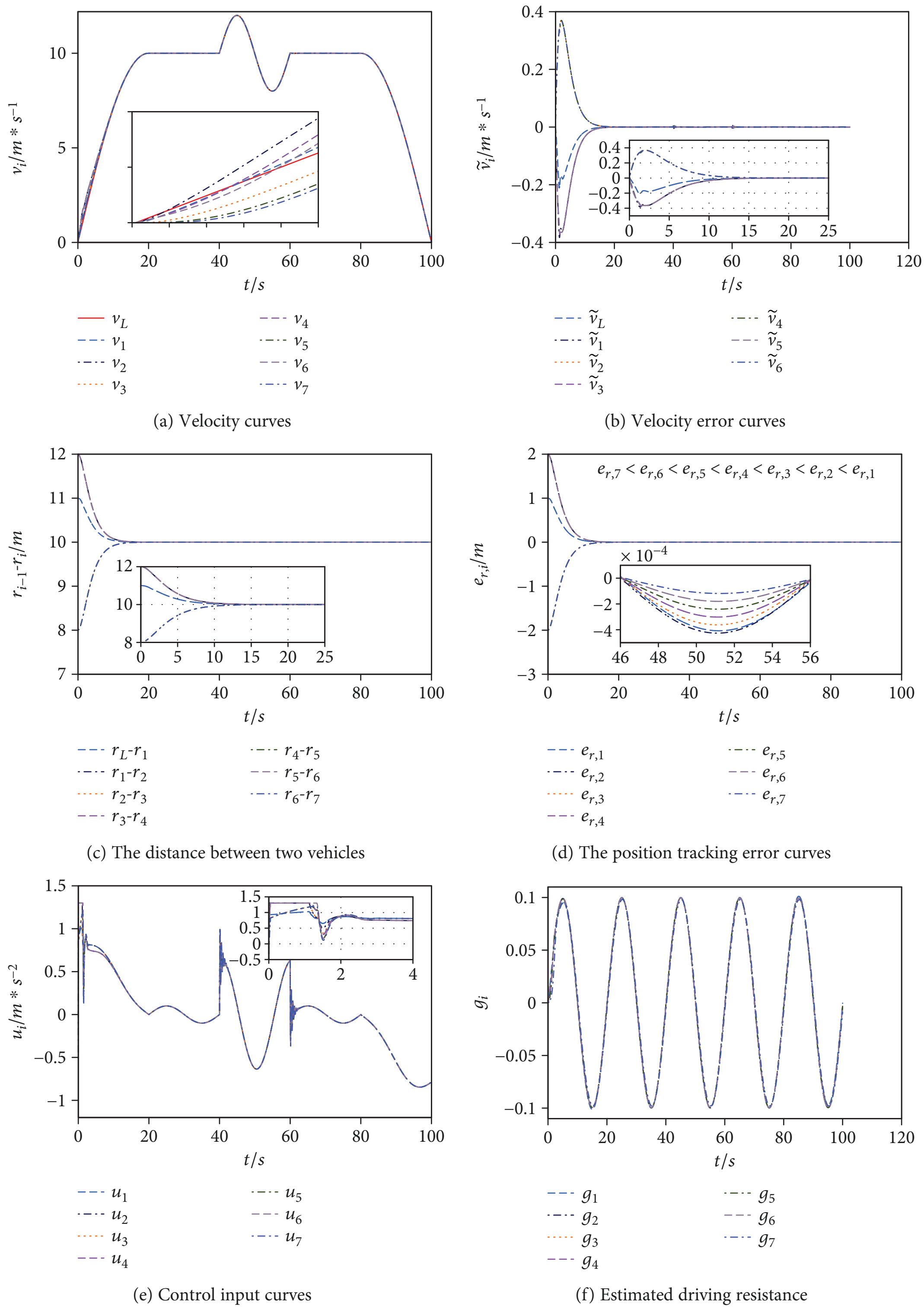

(a) Velocity curves

(b) Velocity error curves

(c) The distance between two vehicles

(d) The position tracking error curves

(e) Control input curves

(f) Estimated driving resistance

Figure 2: Vehicle platoon control with velocity constraints and input saturation.

Actually, the main sources to solve the problems of velocity constraints and input saturation are the signal $\chi_i(t)$ and $\delta_i(t)$. The function of the signal $\chi_i(t)$ is that it can make all the system states on the sliding hyperplane at the initial instant. As a result, the reaching phase of the sliding-mode control is eliminated as well as the transient response of the system is improved (reduce adjustment error in the beginning). The function of the signal $\delta_i(t)$ is that it can attenuate the integral windup of the control law when input saturation or velocity constraints occur. In case of input saturation or velocity constraints ($v_{i0} - v_i \neq 0$ or $u_{i0} - u_i \neq 0$), the signal S_i will rise and the constructed

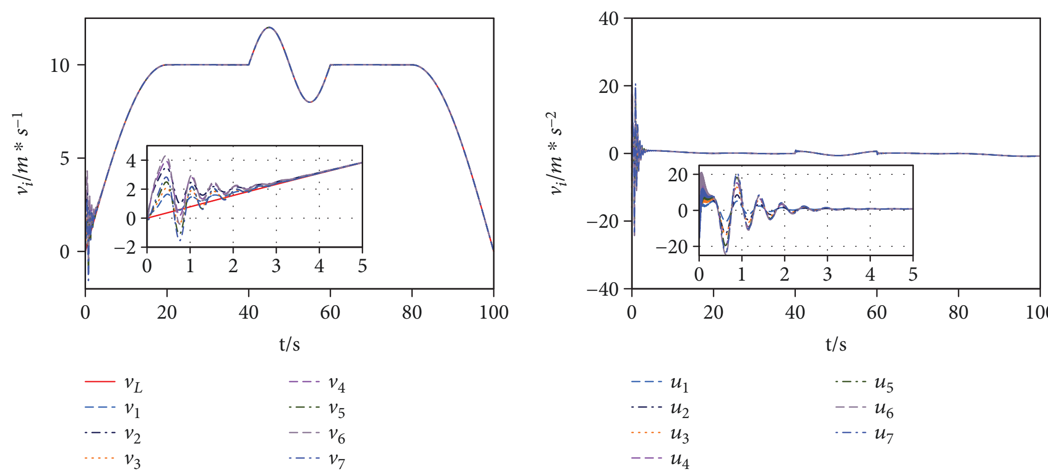

(a) Velocity curves

(b) Control input curves

Figure 3: Vehicle platoon control without input saturation and velocity constrains.

signal $\phi_i(t)$ will also rise, which, in turn, ensures that the newly defined tracking error $\delta_i(t)$ cannot rise abruptly.

Case 2. Vehicle platoon control without input saturation and velocity constraints.

In this part, we further track the same desired velocity curves in (43) by adopting the other related method, which has not taken the input saturation and velocity constraints into consideration. Comparing the numerical simulation results using the method in this case, the control algorithm proposed in this paper can effectively solve the problems of velocity constraints and input saturation.

Figure 3(a) shows the velocity tracking performance by adopting the control algorithm, which has not taken the input saturation and velocity constraints into consideration. The velocities of the vehicles reach negative values in Figure 3(a), which is unreasonable in practical applications. In addition, as shown in Figure 3(b), the control input goes up to $-20\,\mathrm{m/s^2}$ and $20\,\mathrm{m/s^2}$, which cannot be used in application due to the physical structure limitations.

Therefore, the vehicle platoon control algorithm proposed in this paper is more practical and pragmatic.

5. Conclusion

This paper considered the vehicle platoon control problems with velocity constraints and input saturation. Firstly, RBF NNs were introduced to learn the unknown driving resistance. Next, an anti-windup compensation method was designed to avoid the tracking error rising abruptly when velocity constraints or input saturation occurred. Then, a neural adaptive sliding-mode control algorithm was proposed based on bidirectional topology. The string stability and the strong string stability of the whole platoon system were guaranteed. Numerical simulations were performed to verify the feasibility and effectiveness of the proposed control methods.

Data Availability

The data used to support the findings of this paper are available from the corresponding author upon request. All data are included within the manuscript.

Conflicts of Interest

The authors declare that they have no conflicts of interest.

Acknowledgments

This work was partially supported by the National Nature Science Foundation of China (Grant/Award No. 61803040), the Key Science and Technology Program of Shaanxi Province (Nos. 2017JQ6060 and 2018JQ6098), the China Postdoctoral Science Foundation (No. 2017M613030), and the Fundamental Research Funds for the Central Universities of China (Nos. 300102328403, 310832163403, and 310832171004).

References

[1] B. Liu, D. Jia, K. Lu, D. Ngoduy, J. Wang, and L. Wu, "A joint control–communication design for reliable vehicle platooning in hybrid traffic," *IEEE Transactions on Vehicular Technology*, vol. 66, no. 10, pp. 9394–9409, 2017.

[2] B. Besselink and K. H. Johansson, "String stability and a delay-based spacing policy for vehicle platoons subject to disturbances," *IEEE Transactions on Automatic Control*, vol. 62, no. 9, pp. 4376–4391, 2017.

[3] M. di Bernardo, A. Salvi, and S. Santini, "Distributed consensus strategy for platooning of vehicles in the presence of time-varying heterogeneous communication delays," *IEEE Transactions on Intelligent Transportation Systems*, vol. 16, no. 1, pp. 102–112, 2015.

[4] M. di Bernardo, P. Falcone, A. Salvi, and S. Santini, "Design, analysis, and experimental validation of a distributed protocol for platooning in the presence of time-varying heterogeneous

delays," *IEEE Transactions on Control Systems Technology*, vol. 24, no. 2, pp. 413–427, 2016.

[5] L. Alvarez and R. Horowitz, "Safe platooning in automated highway systems part I: safety regions design," *Vehicle System Dynamics*, vol. 32, no. 1, pp. 23–55, 1999.

[6] J. Lygeros, D. N. Godbole, and M. Broucke, "A fault tolerant control architecture for automated highway systems," *IEEE Transactions on Control Systems Technology*, vol. 8, no. 2, pp. 205–219, 2000.

[7] X. Y. Lu and J. K. Hedrick, "A panoramic view of fault management for longitudinal control of automated vehicle platooning," in *ASME 2002 International Mechanical Engineering Congress and Exposition*, pp. 723–730, New Orleans, LA, USA, 2002.

[8] J. Zhou and H. Peng, "Range policy of adaptive cruise control vehicles for improved flow stability and string stability," *IEEE Transactions on Intelligent Transportation Systems*, vol. 6, no. 2, pp. 229–237, 2005.

[9] G. J. L. Naus, R. P. A. Vugts, J. Ploeg, M. J. G. van de Molengraft, and M. Steinbuch, "String-stable CACC design and experimental validation: a frequency-domain approach," *IEEE Transactions on Vehicular Technology*, vol. 59, no. 9, pp. 4268–4279, 2010.

[10] W. B. Dunbar and D. S. Caveney, "Distributed receding horizon control of vehicle platoons: stability and string stability," *IEEE Transactions on Automatic Control*, vol. 57, no. 3, pp. 620–633, 2012.

[11] S. Knorn, A. Donaire, J. C. Agüero, and R. H. Middleton, "Passivity-based control for multi-vehicle systems subject to string constraints," *Automatica*, vol. 50, no. 12, pp. 3224–3230, 2014.

[12] Y. Zheng, S. E. Li, K. Li, and L. Y. Wang, "Stability margin improvement of vehicular platoon considering undirected topology and asymmetric control," *IEEE Transactions on Control Systems Technology*, vol. 24, no. 4, pp. 1253–1265, 2016.

[13] G. Guo and W. Yue, "Hierarchical platoon control with heterogeneous information feedback," *IET Control Theory & Applications*, vol. 5, no. 15, pp. 1766–1781, 2011.

[14] Y. Pan, C. Yang, L. Pan, and H. Yu, "Integral sliding mode control: performance, modification and improvement," *IEEE Transactions on Industrial Informatics*, vol. 14, no. 7, pp. 3087–3096, 2018.

[15] R. Cui, L. Chen, C. Yang, and M. Chen, "Extended state observer-based integral sliding mode control for an underwater robot with unknown disturbances and uncertain nonlinearities," *IEEE Transactions on Industrial Electronics*, vol. 64, no. 8, pp. 6785–6795, 2017.

[16] S. C. Warnick and A. A. Rodriguez, "A systematic antiwindup strategy and the longitudinal control of a platoon of vehicles with control saturations," *IEEE Transactions on Vehicular Technology*, vol. 49, no. 3, pp. 1006–1016, 2000.

[17] G. Makihara, M. Yokomichi, and M. Kono, "Design of nonlinear controllers for active vehicle suspension with state constraints," *Artificial Life and Robotics*, vol. 13, no. 1, pp. 41–44, 2008.

[18] H. Wang, D. Wang, and Z. Peng, "Adaptive dynamic surface control for cooperative path following of marine surface vehicles with input saturation," *Nonlinear Dynamics*, vol. 77, no. 1-2, pp. 107–117, 2014.

[19] D. H. Nguyen, T. Narikiyo, and M. Kawanishi, "Multi-agent system consensus under input and state constraints," in *2016 European Control Conference (ECC)*, pp. 537–542, Aalborg, Denmark, 2017, IEEE.

[20] J. Wu, B. Su, J. Li, X. Zhang, X. Li, and W. Chen, "Adaptive fuzzy control for full states constrained systems with nonstrict-feedback form and unknown nonlinear dead zone," *Information Sciences*, vol. 376, no. 10, pp. 233–247, 2017.

[21] P. Huang, F. Zhang, J. Cai, D. Wang, Z. Meng, and J. Guo, "Dexterous tethered space robot: design, measurement, control and experiment," *IEEE Transactions on Aerospace and Electronic Systems*, vol. 53, no. 3, pp. 1452–1468, 2017.

[22] F. Zhang and P. Huang, "Releasing dynamics and stability control of maneuverable tethered space net," *IEEE/ASME Transactions on Mechatronics*, vol. 22, no. 2, pp. 983–993, 2017.

[23] Y. Li, S. Tong, and T. Li, "Direct adaptive fuzzy backstepping control of uncertain nonlinear systems in the presence of input saturation," *Neural Computing and Applications*, vol. 23, no. 5, pp. 1207–1216, 2013.

[24] C. Wen, J. Zhou, Z. Liu, and H. Su, "Robust adaptive control of uncertain nonlinear systems in the presence of input saturation and external disturbance," *IEEE Transactions on Automatic Control*, vol. 56, no. 7, pp. 1672–1678, 2011.

[25] Y. Li, S. Tong, and T. Li, "Composite adaptive fuzzy output feedback control design for uncertain nonlinear strict-feedback systems with input saturation," *IEEE Transactions on Cybernetics*, vol. 45, no. 10, pp. 2299–2308, 2015.

[26] W. Ren, "On consensus algorithms for double-integrator dynamics," in *2007 46th IEEE Conference on Decision and Control*, pp. 2295–2300, New Orleans, LA, USA, 2008, IEEE.

[27] A. Abdessameud and A. Tayebi, "On consensus algorithms for double-integrator dynamics without velocity measurements and with input constraints," *Systems & Control Letters*, vol. 59, no. 12, pp. 812–821, 2010.

[28] M. Polycarpou, J. Farrell, and M. Sharma, "On-line approximation control of uncertain nonlinear systems: issues with control input saturation," in *Proceedings of the 2003 American Control Conference, 2003*, pp. 543–548, Denver, CO, USA, 2005, IEEE.

[29] S. Li, L. Yang, and Z. Gao, "Adaptive coordinated control of multiple high-speed trains with input saturation," *Nonlinear Dynamics*, vol. 83, no. 4, pp. 2157–2169, 2016.

[30] A. Nedic, A. Ozdaglar, and P. A. Parrilo, "Constrained consensus and optimization in multi-agent networks," *IEEE Transactions on Automatic Control*, vol. 55, no. 4, pp. 922–938, 2010.

[31] P. Lin and W. Ren, "Constrained consensus in unbalanced networks with communication delays," *IEEE Transactions on Automatic Control*, vol. 59, no. 3, pp. 775–781, 2014.

[32] Z. X. Liu and Z. Q. Chen, "Discarded consensus of network of agents with state constraint," *IEEE Transactions on Automatic Control*, vol. 57, no. 11, pp. 2869–2874, 2012.

[33] M. Wang and K. Uchida, "Consensus problem in multi-agent systems with communication channel constraint on signal amplitude," *SICE Journal of Control, Measurement, and System Integration*, vol. 6, no. 1, pp. 7–13, 2013.

[34] S. Gao, B. Ning, and H. Dong, "Adaptive neural control with intercepted adaptation for time-delay saturated nonlinear systems," *Neural Computing and Applications*, vol. 26, no. 8, pp. 1849–1857, 2015.

[35] C. Yang, K. Huang, H. Cheng, Y. Li, and C. Y. Su, "Haptic identification by ELM-controlled uncertain manipulator," *IEEE Transactions on Systems, Man, and Cybernetics: Systems*, vol. 47, no. 8, pp. 2398–2409, 2017.

[36] J. W. Kwon and D. Chwa, "Adaptive bidirectional platoon control using a coupled sliding mode control method," *IEEE*

Transactions on Intelligent Transportation Systems, vol. 15, no. 5, pp. 2040–2048, 2014.

[37] X. Guo, J. Wang, F. Liao, and R. S. H. Teo, "Distributed adaptive integrated-sliding-mode controller synthesis for string stability of vehicle platoons," *IEEE Transactions on Intelligent Transportation Systems*, vol. 17, no. 9, pp. 2419–2429, 2016.

[38] S.-G. Gao, H. R. Dong, B. Ning, C. Roberts, L. Chen, and X. B. Sun, "Cooperative adaptive bidirectional control of a train platoon for efficient utility and string stability," *Chinese Physics B*, vol. 24, no. 9, article 090506, 2015.

[39] X. Liu, C. Yang, Z. Chen, M. Wang, and C. Y. Su, "Neuro-adaptive observer based control of flexible joint robot," *Neurocomputing*, vol. 275, no. 1, pp. 73–82, 2018.

[40] Y. Jiang, C. Yang, J. Na, G. Li, Y. Li, and J. Zhong, "A brief review of neural networks based learning and control and their applications for robots," *Complexity*, vol. 2017, Article ID 1895897, 14 pages, 2017.

[41] G. Guo and W. L. Yuan, "Bidirectional platoon control of Arduino cars with actuator saturation and time-varying delay," *Journal of Control Engineering and Applied Informatics*, vol. 19, no. 1, pp. 37–48, 2017.